Living on the edge: genetic structure and geographic distribution in the threatened Markham's Storm-Petrel (*Hydrobates markhami*)

Heraldo V Norambuena [Corresp., 1, 2, 3] , **Reinaldo Rivera** [2, 4] , **Rodrigo Barros** [3] , **Rodrigo Silva** [3] , **Ronny Peredo** [3] , **Cristián E Hernández** [2, 5]

1 Centro Bahía Lomas, Facultad de Ciencias, Universidad Santo Tomás, Concepción, Chile

2 Laboratorio de Ecología Evolutiva y Filoinformática, Departamento de Zoología, Facultad de Ciencias Naturales y Oceanográficas, Universidad de Concepción, Concepción, Chile

3 Red de Observadores de Aves y Vida Silvestre de Chile, Santiago, Chile

4 Millennium Institute of Oceanography (IMO), Universidad de Concepción, Concepción, Chile

5 Universidad Católica de Santa María, Arequipa, Perú

Corresponding Author: Heraldo V Norambuena
Email address: buteonis@gmail.com

Migratory birds are threatened by habitat loss and degradation, illegal killings, ineffective conservation policies, knowledge gaps and climate change. These threats are particularly troubling in the Procellariiformes (Aves), one of the most endangered bird groups. For "storm-petrels", their cryptic breeding behavior, asynchrony between populations, and light pollution pose additional threats that contribute to increased mortality. Markham's Storm-Petrel (*Hydrobates markhami*), a poorly known migratory species, is a pelagic bird that breeds in dispersed colonies in the Sechura and Atacama Deserts, with asynchronous reproduction between colonies, and is highly affected by artificial lights. Considering its complex conservation scenario and singular breeding, we expected to find narrow habitat distribution conditions, strong geographic genetic structure, and spatially differentiation related to human population activities (e.g. light pollution) and the climate global change. To evaluate these predictions, we analyzed the phylogeography, current and future potential distribution based on mitochondrial gene ND1 and geographic records. The phylogeographic analyses revealed three well-supported clades (i.e. Paracas, Arica, and Salar Grande), and the geographical distribution modeled using an intrinsic conditional model (iCAR) suggests a positive relationship with the mean temperature of the wettest quarter and of the driest quarter, solar radiation, and anthropogenic disturbance. The future predictions under moderate and severe scenarios of global change indicated a drastic distribution area reduction, especially in the southern zone around Tarapacá and Antofagasta in Chile. These suggest a potential loss of unique genetic diversity and the need for conservation actions particularly focused at the edges of the *H. markhami*

distribution.

1 Living on the edge: genetic structure and geographic distribution in the threatened Markham's

2 Storm-Petrel (*Hydrobates markhami*)

3 Heraldo V. Norambuena[1,2, 3,*], Reinaldo Rivera[2,4], Rodrigo Barros[3], Rodrigo Silva[3], Ronny

4 Peredo[3] & Cristián E. Hernández[2,5]

5 [1] Centro Bahía Lomas, Facultad de Ciencias, Universidad Santo Tomás, Concepción, Chile.

6 [2]Laboratorio de Ecología Evolutiva y Filoinformática, Departamento de Zoología, Facultad de

7 Ciencias Naturales y Oceanográficas, Universidad de Concepción, Casilla 160-C, Concepción,

8 Chile.

9 [3]Red de Observadores de Aves y Vida Silvestre de Chile, Santiago, Chile.

10 [4]Millennium Institute of Oceanography (IMO), Universidad de Concepción, Concepción, Chile.

11 [5]Universidad Católica de Santa María, Arequipa, Perú.

13 Corresponding Author:

14 Heraldo V. Norambuena[1,2,3]

16 E-mail address: buteonis@gmail.com

17 **ABSTRACT**

18 Migratory birds are threatened by habitat loss and degradation, illegal killings, ineffective

19 conservation policies, knowledge gaps and climate change. These threats are particularly

20 troubling in the Procellariiformes (Aves), one of the most endangered bird groups. For "storm-

21 petrels" in particular, their cryptic breeding behavior, asynchrony between populations, and light

22 pollution pose additional threats that contribute to increased mortality. Markham's Storm-Petrel

23 (*Hydrobates markhami*), a poorly known migratory species, is a pelagic bird that breeds in

24 dispersed colonies in the Sechura and Atacama Deserts, with asynchronous reproduction

25 between colonies, and is highly affected by artificial lights. Considering its complex

26 conservation scenario and singular breeding, we expected to find narrow habitat distribution

27 conditions, strong geographic genetic structure, and spatially differentiation related to human

28 population activities (e.g. light pollution) and the climate global change. To evaluate these

29 predictions, we analyzed the phylogeography, current and future potential distribution based on

30 mitochondrial gene ND1 and geographic records. The phylogeographic analyses revealed three

31 well-supported clades (i.e. Paracas, Arica, and Salar Grande), and the geographical distribution

32 modeled using an intrinsic conditional model (iCAR) suggests a positive relationship with the

33 mean temperature of the wettest quarter and of the driest quarter, solar radiation, and

34 anthropogenic disturbance. The future predictions under moderate and severe scenarios of global

35 change indicated a drastic distribution area reduction, especially in the southern zone around

36 Tarapacá and Antofagasta in Chile. These suggest a potential loss of unique genetic diversity and

37 the need for conservation actions particularly focused at the edges of the *H. markhami*

38 distribution.

INTRODUCTION

Seabird populations are threatened by the loss and degradation of breeding and non-breeding

habitats, illegal killings, and climate change (Bairlein, 2016; Studds et al., 2017; Wilson et al.,

2018; Xu et al., 2019), which have induces steep declines in abundance and distribution at broad

scales. This problem is only exacerbated by inefficient conservation policies that do not consider

the conservation of breeding sites during the development of investment projects

(Syroechkovskiy 2006; de Boer et al., 2011), and major knowledge gaps in many species' basic

biology, especially in poor countries and for small-bodied species (Rodriguez et al., 2019). This

is particularly troubling on one of the most endangered avian groups, the Procellariiformes

(Class Aves) (Croxall et al., 2012), which are disproportionately threatened compared to Aves

overall (Rodriguez et al., 2019). For the "storm-petrels" this is not only because of its small size,

but also because of its cryptic breeding behavior (i.e., nocturnal colony visits, underground

nesting, remote and inaccessible reproduction areas), high mobility that in some cases, prevent

their study, management, and conservation (Brooke, 2018), and broad distribution that puts them

under different regulations of many national and international jurisdictions and boundaries

(Harrison et al., 2018). All these characteristics contribute to a high vulnerability of breeding

storm-petrels to anthropogenic disturbances. Additionally, one of the main threats at storm-petrel

breeding habitat are light pollution (e.g. Rodríguez et al., 2017). Especially for species with

small, restricted breeding grounds near human populations, where light pollution induces high

mortality of fledglings (e.g. Gineste et al., 2016).

The Markham's Storm-Petrel (*Hydrobates markhami*) is one of the least known

migratory seabirds in the world (Croxall et al., 2012; BirdLife International 2019). However,

artificial light from large cities near breeding areas are known to cause mortality from collision

62   impacts and indirectly from predation by vultures on grounded individuals (Barros et al., 2019).

63   This small pelagic species (21-23 cm) is found mainly in tropical waters of the Pacific Ocean,

64   between 5°N and 29.9°S, and 71°W and 118.02°W (Murphy, 1936; Spear and Ainley, 2007;

65   Howell and Zufelt, 2019). *Hydrobates markhami* is a colonial breeder, with five known

66   dispersed colonies in the Sechura and Atacama Deserts, specifically in saline areas (i.e. salt flats)

67   where they use fissures and cavities found under the surface on the salt flats for nesting,

68   displaying strong philopatry to their natal colonies and nesting sites (Jahncke 1993, 1994,

69   Torres-Mura and Lemus 2013, Schmitt et al. 2015, Barros et al. 2019). The northernmost colony

70   is in Paracas, Peru, where the species breeds in small, dispersed colonies up to 5 km from the sea

71   on the sloping ground (Jahncke, 1993, 1994). The other four colonies are in Chile, located in the

72   Coastal Atacama Desert at up to 50 km inland (Fig. 1; Barros et al., 2019; Medrano et al., 2019).

73   In Chile, the known colonies are (1) Arica, (2) Pampa de la Perdiz, (3) Salar Grande and (4)

74   Salar Navidad (Medrano et al., 2019). Reproduction is asynchronous between colonies (Barros et

75   al., 2019; Medrano et al., 2019). In the northern colonies in Paracas and Arica, most pairs lay

76   eggs between April and August, and chicks hatch asynchronously from July to January with a

77   peak between July and September (Jahnke, 1994; Barros et al., 2019; Medrano et al., 2019).

78   While in the colonies of Pampa Perdiz, Salar Grande and Salar Navidad breeding pairs lay eggs

79   between November and January, and chicks hatch between January and April (Barros et al.,

80   2019; Medrano et al., 2019). The species population size is estimated at 2,305–4,362 breeding

81   pairs in Peru (Jahncke, 1993, 1994) and 55,308–55,733 breeding pairs in Chile (Barros et al.,

82   2019; Medrano et al., 2019). IUCN consider *H. markhami* as Near Threatened (NT; BirdLife

83   International, 2019), but under Chilean classification, this species is categorized as Endangered

84 (EN) due to decreasing population size and extended threats over the breeding colonies (Barros

85 et al., 2019; Medrano et al., 2019).

86   Currently, the genetic data and species distribution modeling could provide important

87 insights for conservation management of *H. markhami*, by examining the relationship between

88 the environment and the species distribution (Humpries et al., 2012; Field et al., 2020).

89 Additionally, it is important to include future scenarios in these combined analyses, given that

90 for many threatened species it has been suggested that their distribution under climate change

91 scenarios will experience important changes, due to translocation of habitat optima (Pecl et al.,

92 2017; Beaumont et al., 2019; Field et al., 2020) or drastic reductions in habitat suitability

93 (Cianfrani et al., 2018; Borges et al., 2019). Considering its complex conservation scenario and

94 the singular breeding habitat geography between colonies and the strong philopatry in *H.*

95 *markhami* (i.e. reproductive isolation and low migration) we expected to find narrow habitat

96 distribution conditions, strong genetic geographic structure, and spatially differentiation related

97 to human population activities (e.g. light pollution) and the climate global change. Under the

98 climate change context, species with unique life history traits are expected to experience more

99 changes in their distribution, which could even lead to loss of genetic diversity (Loarie et al.,

100 2009; Pecl et al., 2017). The aims of this study were to: (1) evaluate the phylogeographic

101 structure and genetic diversity distribution across most of *H. markhami* distributional breeding

102 range; (2) evaluate the effect of climatic variables and anthropogenic impact proxies on the *H.*

103 *markhami* geographic distribution using ecological niche modeling in a Bayesian framework; (3)

104 quantitatively assess the vulnerability to climate change under two representative concentration

105 paths (RCP) of greenhouse gas emissions, which correspond to future climate condition

106 trajectories; and (4) evaluate the effect of migration capacity on the spatial distribution models.

107

MATERIALS AND METHODS

Phylogenetic analysis

110 Between November 12, 2018 and December 01, 2019, we collected blood samples from seven

111 specimens of *H. markhami* from Pampa Chaca, Arica (18°70'S, 70°24'W) and 9 specimens from

112 Salar Grande (21°01'55''S, 69°59'13''W) under permits from Servicio Agrícola Ganadero,

113 SAG, of Chilean government (N°5022/2014 and 5742/2016). DNA was extracted from frozen

114 samples following the protocol of Fetzner (1999) using the QIAGEN DNAeasy kit. We

115 amplified the mitochondrial gene NADH dehydrogenase subunit I (ND1), via polymerase chain

116 reaction (PCR). PCR was performed in a total volume of 25 μL containing 12.5 μL Thermo

117 Scientific PCR Master Mix (0.05 U/μL Taq DNA polymerase, reaction buffer, 4 mM MgCl2, 0.4

118 mM of each dNTP), 0.2 μM of each primer and 20 ng of template DNA. Amplification was

119 performed using the forward TMET-forward: 5'ACC-AAC-ATT-TTC-GGG-GTA-TGG-G 3'

120 and the reverse primer 16DR-reverse: 5'CTA-CGT-GAT-CTG-AGTT-CAG-ACC-GGA-G 3'

121 (Leaché and Reeder, 2002). The following thermal cycler settings were used to amplify all

122 reactions: 5 min at 94°C followed by 35 cycles of 94°C for 30 s, 55°C for 30 s, and 72°C for 30

123 s, followed by a final extension of 72°C for 5 min (Sausner et al., 2007). PCR products were

124 sequenced in both directions through automatic sequencing using Macrogen's ABI3730XL

125 (Seoul, South Korea). Sequences were edited using Codon Code Aligner v. 3.0.3 (CodonCode

126 Corporation, www.codoncode.com), and translated into amino acids to corroborate the absence

127 of stop codons. We got a total of eight sequences with high quality for the analysis (MZ768852

128 to MZ768859; Table S1). Moreover, five ND1 sequences from Paracas breeding site in Cerro

129 Lechuza, Peru (13°8'S, 76°8'W), and one sequence from Chaca in Arica, Chile (18°S, 70°W)

130   were obtained from Sausner et al., (2017) in GenBank (Table S1). In order to avoid obtaining

131   spurious outcomes resulting from the lost phylogenetic information due to substitution

132   saturation, we tested whether the sequences used were useful for the phylogenetic analysis

133   through Xia's test (Xia et al., 2003) implemented in DAMBE v7 (Xia, 2018). Xia's test is an

134   entropy-based index that estimates a substitution saturation index (Iss) in relation to a critical

135   substitution saturation index (Iss.c), by using a randomization process with confidence intervals

136   (95%). The proportion of invariable sites for this analysis was determined in jModeltest 2

137   (Darriba et al., 2012). The sequences of *H. markhami* are available in GenBank according to the

138   accession numbers provided in Table S1. As outgroups in the phylogenetic analyses, we used: *H.*

139   *melania*, *H. microsoma*, *H. tethys*, *H. hornbyi*, *H. leucorhoa* and *H. homochroa*; representatives

140   of Oceanitidae *Oceanites gracilis* and *Fregetta grallaria*; Diomedidae *Thalassarche*

141   *chrysostoma*, *Thalassarche melanophrys* and *Phoebastria nigripes*; and Procellariidae

142   *Aphrodroma brevirostris* (Table S1.).

143   Data were analyzed as previously described in Norambuena et al., (2018), we used both

144   Bayesian inference (BI) and maximum likelihood (ML) approaches for phylogenetic

145   reconstruction. We conducted Bayesian analyses using BEAST v. 1.10.4 program (Drummond et

146   al., 2012), using 'Yule speciation process' for the tree prior to consider the effect of divergent

147   sequences on outgroups (Drummond et al., 2012). We identified the best-fit nucleotide

148   substitution model using jModeltest 2 (Darriba et al., 2012), which indicated HKY+ Γ as the

149   best-fit model for ND1 using BIC and AICc criterion. We ran all analyses for 100 million

150   generations, and we sampled every 1,000 steps; the first 25% of the data was discarded as burn-

151   in. The convergence of MCMC analysis was examined visually in Tracer v1.6 (Rambaut and

152   Drummond, 2009).

153   ML analyses were conducted in RAxML v8 (Stamatakis, 2014) using the multiple

154   inference strategy. We ran 1,000 independent inferences and 1,000 bootstrap replicates with the

155   same nucleotide substitution model settings as for the Bayesian analysis. Support values from

156   1,000 bootstrap replicates were annotated on the tree with the highest likelihood. .

157   We also inferred a haplotype network as previously described in Norambuena et al.,

158   (2018) by using the "median joining network" algorithm in Network 4.610 (Bandelt et al., 1999),

159   which is based on the sum of weighted differences (i.e. Hamming distance) between sequences.

160   Ambiguities within the network were solved according to the criteria of Crandall and Templeton

161   (1993). Finally, for each geographic area (i.e. Paracas, Arica and Salar Grande) retrieved by

162   phylogenetic analysis, we calculated in DnaSP v.5 (Librado and Rozas, 2009) the number of

163   polymorphic sites (S), haplotype diversity (H) and nucleotide diversity (Π).

164

165   **Occurrence data and climate variables**

166   *Hydrobates markhami* occurrence data were obtained during 12 expeditions (see Barros et al.,

167   2019 for details), literature from the Peruvian colonies (e.g. Jahncke 1993, 1994; Torres-Mura

168   and Lemus, 2013), and electronic databases (eBird, 2020). We obtained a total of 972

169   georeferenced records that were later reduced to 75 data cleaning (Supplemental Data S1). All

170   the final records correspond to confirmed and potential nests on breeding sites (Jahncke 1993,

171   1994; Barros et al., 2019). To reduce spatial autocorrelation that usually results from sampling

172   areas with a high density of locality points (clusters of points), we spatially filtered locality data

173   to allow a minimum distance of 1 kilometer between any two points.

174   The climatic variables were obtained from Wordclim version 2.1 with 2.5 minutes spatial

175   resolution (Fick and Hijmans, 2017). Additionally, we obtained environmental variables such as

176 ultraviolet radiation (Beckmann et al., 2014), elevation, wind (Fick and Hijmans, 2017) and

177 topographic roughness (Amatulli et al., 2018). As anthropogenic impact proxies, we used the

178 databases of Human footprint (Venter et al., 2016), artificial lights (Falchi et al., 2016) and

179 human population (CIESIN, 2016). We selected the variables that were used in the models

180 through an exploratory analysis which resulted in strongly correlated variables to be eliminated.

181 We used the variance inflation factor (VIF) to evaluate the collinearity among predictors, where

182 VIF greater than 10 is a signal that the model has collinearity problems (Quinn and Keough,

183 2002). Our analyzes showed that four variables have a VIF <3 and four variables have a VIF

184 between 4 and 9, which are below the threshold (VIF <10) (See Fig. S1 and Table S2). Finally,

185 eight uncorrelated variables were used to perform the species distribution models (SDMs): Min

186 Temperature of Coldest Month, Temperature Annual Range, Mean Temperature of Wettest

187 Quarter, Mean Temperature of Driest Quarter, Human footprint, artificial lights, solar radiation,

188 and wind (see Table S2).

189

190 **Species distribution modelling (SDM)**

191 The geographical distribution of *H. markhami* was modeled using an intrinsic conditional model

192 (iCAR). We assume that the response variable *Zi* is a binary variable that represents the presence

193 (1) or absence (0) of *H. markhami*. This approach explicitly considers spatial autocorrelation

194 (Latimer et al., 2006) to adjust an ecological process where the presence/absence of the species is

195 explained by the suitability of the habitat (Vieilledent et al., 2014), where:

196 $Z_i \sim$ Bernoulli (π_i)

197 logit $(\pi_i) = X_i\beta + \rho_{j(i)}$

198   X_i= matrix of covariates, β= vector of the regression coefficients, ρ represents the random spatial

199   effect of the observation i in cell j, and the logit link is used to model the relationship between π_i,

200   the covariates and spatial effect. Models were built using the package "hSDM" (Vieilledent,

201   2019) in the software R (Core Team 2019). Uninformative priors centered at zero with a fixed

202   large variance of 100 were used for all parameters involved in both ecological and observation

203   processes, while a uniform distribution was used for the variance of the spatial effects (Pennino

204   et al., 2017). We chose the model which had the lowest Deviance Information Criterion (DIC)

205   (Spiegelhalter et al., 2002), where lower values of DIC represent the best compromise between

206   fit and estimated number of parameters.

207

208   **Geographical projection to the future scenarios**

209   To model the geographic distribution into the future, we selected two representative

210   concentration paths (RCP) of greenhouse gases, which correspond to future climate conditions

211   trajectories of greenhouse gases adopted by the IPCC (Stocker et al., 2013). RCPs span the range

212   of the year 2100 radiative forcing, i.e. from 2.6 to 8.5 W/m² (van Vuuren et al., 2011). An RCP

213   2.6 was selected as the scenario for an extremely low forcing level and 8.5 as an extremely high

214   baseline emission scenario. Three global climate models (GCMs); CCCMA, CSIRO and MIROC

215   were evaluated for the year and 2080. The climatic projections were obtained from the portal

216   http://www.ccafs-climate.org/ (Navarro et al., 2020). We explored 32 GCMs projections through

217   the GCM compareR application (Fajardo et al. 2020). CCMA, CSIRO represent models where

218   low precipitation and high temperature are represented, while MIROC is a more conservative

219   model and closest to the study area's average (e.g., Alarcón & Cavieres, 2015; Lazo-Cancino et

220   al., 2020). In the future projections of the SDMs, we only use the variables min temperature of

221   the coldest month, temperature annual range, mean temperature of the wettest quarter, and mean

222   temperature of the driest quarter. The variables for Human footprint, artificial lights, radiation

223   and wind were not included since there are no future predictions for these variables.

224   To quantify geographic distribution changes under future climate change scenarios, we

225   compared the current model with future projected models. Each model was converted from a

226   continuous output to a binary classification (presence/absence) using the threshold that

227   maximizes the sum of sensitivity and specificity (max SSS) (Liu et al., 2013). Then the areas

228   gained, lost, no occupancy, and no change in the future were estimated. We calculated the

229   estimated areas in square kilometers using the South American Albers Equal Area Conic

230   projection. We used SDMtoolbox module (Brown, 2014) implemented in ArcGIS 10.4.1 (ESRI,

231   2015) to calculate the areas of expansion range, contraction range, and the distribution without

232   change between present and future models.

233

234   **Migration constraints**

235   Since the SDMs are static in nature and do not consider the species dispersal ability, biotic

236   interactions, or population dynamics (Zurell et al., 2009, 2016; Engler et al., 2012), these do not

237   allow predicting the effect of climate change on the distribution of species in a realistic way.

238   Therefore, in our models, we consider limitations to the dispersion of *H. markhami* in the

239   projections, through the "Migclim" approximation (Engler et al., 2009; Engler et al., 2012). This

240   method explicitly includes the dispersal of a species, potential propagule production, geographic

241   barriers, short-distance dispersal capacity (SDD) and probability for long-distance dispersal

242   (LDD) (Engler et al., 2012). We performed the analyzes using the habitat suitability models

243   predicted by iCAR for the years 2030, 2050 and 2080. Because not all the parameters required

244   by the algorithm are known, we opted to consider a model with barriers to dispersion, using three

245   thresholds (300, 500 and 700), where habitat suitability scales from 0 to 1000, and the values

246   below the threshold are considered absences and above the threshold they are considered

247   presences. These thresholds allow the classification of suitable or unsuitable habitat, where cells

248   with habitat suitability ≥ threshold are considered as suitable, values <threshold unsuitable. We

249   do not consider long-distance dispersion since *H. markhami* is highly philopatric (see results). To

250   set the spatial barriers for future dispersion we consider the Human Footprint as a "strong"

251   barrier, given the sensitivity of this species to human activity. The analyzes were performed for

252   the three global climate models (GCMs); CCCMA, CSIRO and MIROC. We compare the results

253   of each Migclim run selecting the best and worst simulated scenario, as follow: for the best

254   scenario, we consider one with the highest number of occupied cells, the smallest number of

255   absent cells at the end of the dispersion process, and the largest number of cells that could be

256   used in the case of "unlimited dispersal" and "non-dispersal"; and the opposite conditions was

257   considered as the worst scenario. The analyzes were performed in the MigClim 1.6 package

258   (Engler et al., 2013). All simulations for each GCMs and RCP are detailed in Table S3.

259

260   **RESULTS**

261   **Genetic population structure**

262   Sequences of 955 bp in length for the ND1 locus were obtained and the result of Xia's test

263   suggests low saturation, as the critical index of substitution saturation value (Iss.c = 0.819) were

264   significantly higher than the observed index of substitution saturation values (Iss = 0.514; p <

265   0.0001), therefore, the sequences were deemed suitable for performing phylogenetic analyses.

266   Four haplotypes were identified defined by 17 polymorphic sites. The ML and BI trees based on

267   ND1 sequences showed identical topologies (Fig. 1A). Both trees inferred that the *H. markhami*

268   is monophyletic and composed of three well-supported clades (posterior probability pp of 0.9-1.0

269   and ML bootstrap support of 100). The three clades are geographically structured, with one clade

270   represented by Paracas individuals, the other by Arica, and the third by Salar Grande individuals

271   (Fig. 1A). The only geographic incongruence was in the Paracas clade where a sample from

272   Arica was the sister of all the Paracas individuals that are monophyletic with a 0.9 of pp (Fig.

273   1A).

274   The ND1 haplotype network revealed the same three major clades recovered from the BI

275   and ML phylogenies (Fig. 1B). Overall haplotype diversity for the ND1 gene was 0.747 ± 0.004

276   and overall nucleotide diversity was 0.028. The clade of Paracas had the highest haplotype

277   diversity and the clade of Arica had the highest nucleotide diversity, while the clade of Salar

278   Grande had the lowest values and was represented by one exclusive haplotype.

279

280   **Present and future geographic distribution**

281   The *H. markhami* distribution was mainly driven by min temperature of the coldest month (Bio

282   6), temperature annual range (Bio 7), mean temperature of the wettest quarter (Bio 8), mean

283   temperature of the driest quarter (Bio 9), Human footprint (HFP), and radiation (Table 1).

284   Positive relationships were found between Bio 8, Bio 9, HFP, radiation and the occurrence of *H.*

285   *markhami*, and negative relationship with the variables Bio 6 and Bio 7 (Table 1, Fig. S1). The

286   highest median posterior probability of the presence of *H. markhami* occurs around the region of

287   Paracas (Peru), and in a continuous area from the southern coast of Arequipa region in Peru to

288   Antofagasta region in Chile (Fig. 2A). The spatial effect, that is, a model without considering the

289   environmental predictors, showed to be strong for almost the entire modeled distribution range of

290   the species (Fig. 2B). By 2080, the distribution predicted considering less severe scenarios (i.e.,

291   RCP 2.6) and severe (RCP 8.5) showed that expansion areas geographic range were greater than

292   the areas of contraction geographic range (Fig. 3 and Fig. 4) (See Table S3 and Fig. S2). The

293   MIROC model (RCP 2.6) was the only case where there would be a greater contraction of the

294   geographic range predicted in the future (Table S3). In all models and Representative

295   Concentration Pathway, a high no-occupancy geographic area is predicted, that is, areas

296   currently not occupied by the species and that are not expected to be occupied in the future.

297   Similarly, a significant area of no-change is predicted, that is, areas currently occupied by the

298   species and expected to remain occupied in the future (See Table S3 and Figs. S2-5).

299   The habitat changes predicted by the simulations indicate two highly contrasting

300   simulations (Table 2). The first one indicating a low impact on the distribution of the species in a

301   future scenario for the GCMs model MIROC (RCP 2.6) with a high number of pixels that would

302   be colonized at the beginning and end of the simulation, though, there are also numerous areas to

303   the south of their known distribution that would not be colonized (pink pixels) (Fig. 5A, Table

304   2); The second, being the worst case scenario for *H. markhami* (Fig. 5B, Table 2), where the

305   CCMA model (RCP 8.5) indicated a low number of occupied and colonized pixels at the end of

306   the simulation, reducing the number of areas that are suitable in the present and that would also

307   be suitable in the future (red pixels). The remaining simulations by GCMs and RCP support

308   previous results and are shown in Figs. S2-4 of the supplementary materials.

309

310   **Discussion**

311   **Genetic population structure**

312   The phylogeny and haplotype network supported three main lineages within *H. markhami*,

313   showing a clear geographic structure associated to breeding areas in Paracas, Arica and Salar

314   Grande. The shared haplotype between Paracas and Arica suggests some degree of connectivity

315   between both areas (gene flow), however, we cannot discard that could be due to incomplete

316   lineage sorting. This result is coherent with the fact that the northern colonies (Paracas and

317   Arica) share breeding phenology, with most pairs laying eggs between April and August, and

318   chicks hatching from July to January (Jahnke, 1994; Barros et al., 2019; Medrano et al., 2019).

319   On the other hand, the differentiated haplotype from Salar Grande shares breeding phenology

320   with Pampa Perdiz and Salar Navidad, with pairs laying eggs between November and January,

321   and chicks hatching between January and April (Barros et al., 2019; Medrano et al., 2019). This

322   fact supports the importance of breeding phenologies as a key factor in explaining

323   microevolutionary processes in the *Hydrobates* genus. For example, for the *H. castro* species

324   complex, the occurrence of two different phenologies (hot and cold season) has been described

325   as a relevant mechanism for sympatric speciation (Monteiro and Furnes, 1998; Friesen et al.,

326   2007). This strong degree of geographic structure has been documented previously in Peruvian

327   diving-petrel and two Patagonian shag species that breed in colonies along the coasts of Peru,

328   Chile and Argentina (Calderón et al., 2014; Cristofari et al., 2019). However, to test the

329   relevance of the gene flow hypothesis requires additional samples improve our preliminary result

330   about geographic structured pattern and active dispersion between Paracas and Arica.

331   The biological association between breeding phenologies in *H. markhami* and saline areas

332   produce strong philopatry to their natal colonies and nesting sites (Jahncke, 1993, 1994; Torres-

333   Mura and Lemus, 2013; Schmitt et al., 2015; Barros et al., 2019). A large number of studies have

334   now documented that all *Hydrobates* species of South America use salt flats/saltpetre deposits in

335   the coastal deserts of Sechura and Atacama to nest (Jahncke 1993, 1994; Bernal et al., 2006;

336   Ayala et al., 2007; Torres-Mura and Lemus, 2013; Barros et al., 2019; Medrano et al., 2019), and

337   even some *Oceanites* storm-petrels (Oceanitidae family) have been found using the same areas

338   for nesting (Barros et al., 2020).

339

340   **Geographic distribution**

341   Under conservative and more severe climate change scenarios, our models suggest moderate

342   reductions and strong reduction of the distribution of *H. markhami*, respectively, which agree

343   with the idea that species with specialist reproductive habitat (e.g. breeding phenology associated

344   with saline areas) are especially sensitive to the effects of rapid climate-change (Loarie et al.,

345   2009), because of the constraints imposed by this specific requirement for breeding sites (i.e.

346   niche conservatism). To date, after multiple expeditions searching for breeding sites, they have

347   only found *H. markhami* breeding in this specific environment (Barros et al. 2019, Medrano et

348   al. 2020). But considering that some petrels are able to use cavities in other substrates, such as

349   soft soil and man-made burrows (Podolsky & Kress 1989, Bolton et al. 2004), we do not rule out

350   the capability of nest substrate plasticity.

351   The most impacted area of *H. markhami* distribution will be its current southern edge between

352   the Tarapacá and Antofagasta regions in Chile. Moreover, this is also the most affected area by

353   light contamination (see Barros et al., 2019), considering that 11.41% (2.269 MW) of the

354   electrical power of Chile is generated in this area and large cities dependent on mining-related

355   economy (e.g. Iquique and Antofagasta) continue to grow. The future reduction in the

356   distribution of *H. markhami* may be even more severe than suggested by our models, given that

357   we were not able to include a prediction of human footprint in the models.

358   According to our results, the predicted future habitat range of *H. markhami* is likely to be

359   negatively affected by future climate change and will concentrate on the central portion of its

360   present distribution (i.e. around the Arica area). The first response of species to climate change

361   under GCMs MIROC RCP 2.6 scenario would be the colonization of areas around present

362   distribution, but under CCMA model (RCP 8.5) this colonization considerably decreased. In both

363   scenarios the southern distribution would not be colonized and suitable in the future (MigClim

364   simulation, Fig. 5). The MigClim simulations also suggest the loss of some areas in Southern

365   Peru and in the south of Arica colony. Unlike species with greater mobility or fewer restrictions

366   on reproductive habitat, that shift their distributions moving poleward and to higher elevations

367   (Chen et al., 2011; Pecl et al., 2017), the limited distribution of salt flats/saltpetre deposits (Sáez

368   et al., 2012) -key habitat for *H. markhami* nesting- will affect the responses of this species to

369   climate change. This, added to the small population of *H. markhami* (Barros et al., 2019), would

370   constrain its distribution range change by limiting its colonizing capability, and thus increasing

371   its extinction risk.

372   Most research on the response of seabird to climate change has been studies considering

373   at-sea distribution (e.g. Wolf et al., 2010; Humpries et al., 2012). However, for seabirds such as

374   *H. markhami*, the individuals at the breeding colonies could be affected by the warming of air

375   temperature, that in severe cases could cause mortality due to overheating and physiological

376   stress (Sydeman et al., 2012). These last conditions, related to an increase of temperature, could

377   be particularly important in the breeding habitat of *H. markhami* in the Sechura and Atacama

378   Deserts. In fact, it is expected that seabird species will respond differentially to climate change

379   according to many different factors, including life history characteristics, diet, range, and

380   abundance (Furness and Tasker, 2000; Sydeman et al., 2012). So, while some seabirds may fare

381   well in warming oceans, others may become locally, regionally, or perhaps even globally extinct

382   (e.g. Kitaysky and Golubova, 2000; Jenouvrier et al., 2009; Wolf et al., 2010; Lewison et al.,

383   2012).

384

385   **CONCLUSIONS**

386   Overall, our results of *H. markhami* can be useful for the design of conservation policies,

387   considering that the planning of protected areas and management should be focused on areas

388   with higher or unique genetic diversity (Midgley et al., 2003; Ayebare et al., 2018). In *H.*

389   *markhami*, the extinction of any local population could mean a loss of unique genetic diversity.

390   The southern portion of the *H. markhami* distribution (Tarapacá and Antofagasta) are the most

391   vulnerable areas according to our results and do not have any type of legal protection today. The

392   only breeding area partially protected is Paracas in Perú (Jahncke, 1993; 1994). This provides a

393   complex conservation scenario for this species, especially considering the future consequences of

394   climate change. Finally, considering the complex conservation scenario, singular breeding habits,

395   its narrow habitat distribution conditions, preliminary evidence of genetic geographic structure,

396   and spatial differentiation related to human population activities (e.g. light pollution and climate

397   global change); we highlight the urgent need for increased cooperation and governance between

398   the Peruvian and Chilean wildlife technical units, and the protection of their breeding sites in the

399   center and south of their distribution, given that the local extinctions occur closer to the border or

400   core range depending on local and regional environmental factors intermingled with human

401   impacts (Cowlishaw et al., 2009; Boakes et al., 2018).

402

403   **ACKNOWLEDGEMENTS**

404 We thank Fernando Medrano for his comments on drafts of the manuscript. We thank the 'ROC'

405 volunteers that assisted the research and conservation project of Atacama storm-petrels. We

406 thank American Bird Conservancy (ABC) (Grant #B2016-04 and #1854A) for funding and

407 advise for our fieldwork from 2016–2020 and the Mohammed Bin Zayed Fund and the Packard

408 Foundation, for funding our fieldwork in 2017 through ABC. HVN was funded by FONDECYT-

409 POSTDOCTORADO 3190618 and CEH by the FONDECYT 1170815 and 1201506 grants. RR

410 was supported by Millennium Institute of Oceanography (IMO), University of Concepción,

411 Concepción, Chile. We thank an anonymous reviewer and Marcelo Rivadeneira for revisions to

412 the manuscript.

REFERENCES

Alarcón D, Cavieres LA. 2015 In the Right Place at the Right Time: Habitat Representation in

Protected Areas of South American Nothofagus-Dominated Plants after a Dispersal

Constrained Climate Change Scenario. *PLoS ONE* **10(3)**: e0119952.

https://doi.org/10.1371/journal.pone.0119952

Amatulli G, Domisch S, Tuanmu M-N, Parmentier B, Ranipeta A, Malczyk J, Jetz W.

2018. A suite of global, cross-scale topographic variables for environmental and biodiversity

modeling. *Scientific Data* 5, 180040. doi:10.1038/sdata.2018.40.

Ayala L, Sanchez-Scaglioni R. 2007. A new breeding location for the Wedge-rumped Storm-

Petrel *Oceanodroma tethys kelsalli* in Peru. *Journal of Field Ornithology* **78(3)**: 303-307.

Ayebare S, Plumptre AJ, Kujirakwinja D, Segan D. 2018. Conservation of the endemic

species of the Albertine Rift under future climate change. *Biological Conservation* **220**: 67–

75.

Bandelt HJ, Forster P, Röhl A. 1999. Median-joining networks for inferring intraspecific

phylogenies. *Molecular Biology and Evolution* **16**:37–48.

Barros R, Medrano F, Norambuena HV, Peredo R, Silva R, De Groote F, Schmitt F. 2019.

Breeding biology, distribution, and conservation status of Markham's Storm-Petrel

(*Oceanodroma markhami*) in the Atacama Desert. *Ardea* **107**:75–84.

Barros R, Medrano F, Silva R, Schmitt F, Manilarich V, Terán D, Peredo R, Pinto C,

Vallverdú A, Fuchs J, Norambuena HV. 2020. Breeding sites, distribution and conservation

status of the White-vented Storm-petrel (*Oceanites gracilis*) in the Atacama Desert. *Ardea*

108(2): 203–212.

435 **Beaumont LJ, Esperón-Rodríguez M, Nipperess DA, Wauchope-Drumm M, Baumgartner**

436   **JB. 2019.** Incorporating future climate uncertainty into the identification of climate change

437   refugia for threatened species. *Biological Conservation* **237**:230–237.

438   https://doi.org/10.1016/j.biocon.2019.07.013

439 **Beckmann M, Václavík T, Manceur AM, Šprtová L, von Wehrden H, Welk E, Cord AM.**

440   **2014.** glUV: A global UV-B radiation dataset for macroecological studies. *Methods in*

441   *Ecology and Evolution* **5:**372–383.

442 **Bernal M, Simeone A, Flores M. 2006.** Breeding of Wedge-rumped Storm-petrels

443   (*Oceanodroma tethys*) in northern Chile. *Ornitologia Neotropical* **17(2)**:283–287.

444 **BirdLife International. 2019.** *Hydrobates markhami.* The IUCN Red List of Threatened

445   Species 2019: e.T22698543A156377889. https://dx.doi.org/10.2305/IUCN.UK.2019-

446   3.RLTS.T22698543A156377889.en. Downloaded on 27 March 2020.

447 **Boakes EH, Isaac N, Fuller RA, Mace GM, McGowan P. 2018.** Examining the relationship

448   between local extinction risk and position in range. *Conservation Biology* **32(1)**: 229–239.

449 **Bolton M, Medeiros R, Hothersall B, Campos A. 2004.** The use of artificial breeding

450   chambers as a conservation measure for cavity-nesting procellariiform seabirds: a case study

451   of the Madeiran storm petrel (*Oceanodroma castro*). *Biological Conservation* **116:** 73–80.

452 **Brown JL 2014.** SDMtoolbox: a python-based GIS toolkit for landscape genetic, biogeographic

453   and species distribution model analyses. *Methods in Ecology and Evolution* **5**: 694–700.

454 **Carboneras C, Jutglar F, Kirwan GM. 2020.** Black Storm-petrel (*Hydrobates melania*). In:

455   del Hoyo, J., Elliott, A., Sargatal, J., Christie, D.A. & de Juana, E. (eds.). Handbook of the

456   Birds of the World Alive. Lynx Edicions, Barcelona. (retrieved from

457   https://www.hbw.com/node/52598 on 2 April 2020).

458 **CIESIN (Center for International Earth Science Information Network - Columbia**

459 **University). 2016.** Documentation for the Gridded Population of the World, Version 4

460 (GPWv4). Palisades NY: NASA Socioeconomic Data and Applications Center (SEDAC).

461 http://dx.doi.org/10.7927/H4D50JX4 Accessed 01 May 2020.

462 **Crandall KA, Templeton AR. 1993.** Empirical tests of some predictions from coalescent theory

463 with applications to intraspecific phylogeny reconstruction. *Genetics* **134**:959–969.

464 **Cowlishaw G, Pettifor RA, Isaac NJB. 2009.** High variability in patterns of population decline:

465 the importance of local processes in species extinctions. *Proceedings of the Royal Society B-*

466 *Biological Sciences* **276**:63–69.

467 **Darriba D, Taboada GL, Doallo R, Posada D. 2012.** jModelTest 2: more models, new

468 heuristics and parallel computing. *Nature Methods* **9**:772–772.

469 **Drummond AJ, Suchard MA, Xie D, Rambaut A. 2012.** Bayesian phylogenetics with BEAUti

470 and the BEAST 1.8. *Molecular Biology and Evolution* **29**:1969–1973.

471 **eBird. 2020.** eBird: An online database of bird distribution and abundance [web application].

472 eBird, Cornell Lab of Ornithology, Ithaca, New York. Available: http://www.ebird.org.

473 (Accessed: Date [e.g., May 2, 2020]).

474 **Engler R, Randin CF, Vittoz P, Czáka T, Beniston M, Zimmermann NE, Guisan A. 2009.**

475 Predicting future distributions of mountain plants under climate change: does dispersal

476 capacity matter? *Ecography* **32**:34–45.

477 **Engler R, Hordijk W, Guisan A. 2012.** The MIGCLIM R package-seamless integration of

478 dispersal constraints into projections of species distribution models. *Ecography* **35**:872–878.

479 **ESRI 2015.** ArcGIS Desktop: Release 10. Redlands, CA: Environmental Systems Research

480 Institute.

481 **Fajardo J, Corcoran D, Roehrdanz PR, Hannah L, Marquet PA. 2020.** GCM COMPARER:

482   A web application to assess differences and assist in the selection of general circulation

483   models for climate change research. *Methods in Ecology and Evolution* **11**: 656–663.

484 **Falchi F, Cinzano P, Duriscoe D, Kyba CC, Elvidge CD, Baugh K, Portnov BA, Rybnikova**

485   **NA, Furgoni R. 2016.** The new world atlas of artificial night sky brightness. *Science*

486   *Advances* 1:2(6):e1600377.

487 **Fetzner JFC. 1999.** Extracting high-quality DNA from shed reptile skins: a simplified method.

488   *Biotechniques* **26**:7–9.

489 **Fick SE, Hijmans RJ. 2017.** WorldClim 2: new 1km spatial resolution climate surfaces for

490   global land areas. *International Journal of Climatology* **37(12)**: 4302–4315.

491 **Field RH, Buchanan GM, Hughes A, Smith P, Bradbury RB. 2020.** The value of habitats of

492   conservation importance to climate change mitigation in the UK. *Biological Conservation*

493   **248**, [108619]. https://doi.org/10.1016/j.biocon.2020.108619

494 **Friesen VL, Smith AL, Gómez-Díaz E, Bolton M, Furness RW, González-Solís J, Monteiro**

495   **LR. 2007.** Sympatric speciation by allochrony in a seabird. *Proc. Natl. Acad. Sci.* **104**:18589–

496   18594.

497 **Furness RW, Tasker ML. 2000.** Seabird-fishery interactions: quantifying the sensitivity of

498   seabirds to reductions in sandeel abundance, and identification of key areas for sensitive

499   seabirds in the North Sea. *Marine Ecology Progress Series* **202**:253−264

500 **Jahncke J. 1993.** Primer informe del área de anidación de la golondrina de tempestad negra

501   *Oceanodroma markhami* (Salvin 1883). Proc. X Congr. Nac. Biol., 1992. Lima, Perú. pp.

502   339–343.

503   **Jahncke J. 1994.** Biología y conservación de la Golondrina de Tempestad Negra *Oceanodroma*

504   *markhami* (Salvin 1883) en la Península de Paracas, Perú. APECO, Lima.

505   **Jenouvrier S, Caswell H, Barbraud C, Holland M, Stroeve J, Weimerskirch H. 2009**

506   Demographic models and IPCC climate projections predict the decline of an emperor penguin

507   population. *Proc Natl Acad Sci* **106**:1844−1847.

508   **Kitaysky A, Golubova EG. 2000.** Climate change causes contrasting trends in reproductive

509   performance of planktivorous and piscivorous alcids. J*ournal of Animal Ecology* **69**:248−262.

510   **Latimer AM, Wu SS, Gelfand AE, Silander JA. 2006.** Building statistical models to analyze

511   species distributions. *Ecological Applications* **16**:33–50

512   **Lazo-Cancino D, Rivera R, Paulsen-Cortez K, González-Berríos N, Rodríguez-Gutiérrez R,**

513   **Rodríguez-Serrano E. 2020.** The impacts of climate change on the habitat distribution of the

514   vulnerable Patagonian-Fueguian species *Ctenomys magellanicus* (Rodentia, Ctenomyidae).

515   *Journal of Arid Environments* **173**: 104016

516   **Leaché AD, Reeder TW. 2002.** Molecular systematics of the eastern fence lizard (*Sceloporus*

517   *undulatus*): A comparison of parsimony, likelihood, and Bayesian approaches. *Systematic*

518   *Biology* **51**:44–68.

519   **Lewison R, Oro D, Godley B, Underhill L, Bearhop S, Wilson RP, Ainley D, Arcos JM,**

520   **Boersma PD, Borboroglu PG, Boulinier T, Frederiksen M, Genovart M, González-Solís**

521   **J, Green JA, Grémillet D, Hamer KC, Hilton GM, Hyrenbach KD, Martínez-Abraín A,**

522   **Montevecchi WA, Phillips RA, Ryan PG, Sagar P, Sydeman WJ, Wanless S, Watanuki**

523   **Y, Weimerskirch H, Yorio P. 2012.** Research priorities for seabirds: improving conservation

524   and management in the 21st century. *Endangered Species Research* **17**:93−121.

525 **Librado P, Rozas J. 2009.** DnaSP v5: a software for comprehensive analysis of DNA

526   polymorphism data. *Bioinformatics* **25**:1451–1452.

527 **Liu C, White M, Newell G. 2013.** Selecting thresholds for the prediction of species occurrence

528   with presence-only data. *Journal of Biogeography* **40(4)**: 778–789.

529 **Loarie SR, Duffy PB, Hamilton H, Asner GP, Field CB, Ackerly DA. 2009.** The velocity of

530   climate change. *Nature* **462**:1052–1055.

531 **Medrano F, Silva R, Barros R, Terán D, Peredo R, Gallardo B, Cerpa P, De Groote F,**

532   **Gutiérrez P, Tejeda I. 2019.** Nuevos antecedentes sobre la historia natural y conservación de

533   la golondrina de mar negra (*Oceanodroma markhami*) y la golondrina de mar de collar

534   (*Oceanodroma hornbyi*) en Chile. *Revista Chilena de Ornitología* **25(1)**:21–30.

535 **Midgley GF, Hannah L, Millar D, Thuiller W, Booth A. 2003.** Developing regional and

536   species-level assessments of climate change impacts on biodiversity in the Cape Floristic

537   Region. *Biological Conservation* **112**:87–97.

538 **Monteiro LR, Furness RW. 1998.** Speciation through temporal segregation of Madeiran Storm-

539   petrel (*Oceanodroma castro*) populations in Azores? *Phil. Trans. R. Soc. Lond. B* **353**:845

540   –953.

541 **Murphy RC. 1936.** Oceanic birds of South America. Vol. 2. MacMillan Company, New York.

542 **Navarro-Racines C, Tarapues J, Thornton P, Jarvis A, Ramirez-Villegas J. 2020.** High-

543   resolution and bias-corrected CMIP5 projections for climate change impact assessments. *Sci*

544   *Data* **7**, 7, doi:10.1038/s41597-019-0343-8.

545 **Norambuena HV, Van Els P, Muñoz-Ramírez CP, Victoriano PF. 2018.** First steps towards

546   assessing the evolutionary history and phylogeography of a widely distributed Neotropical

547   grassland bird (Motacillidae: *Anthus correndera*). *PeerJ*, **6**, e5886.

548 **Pecl GT, Araújo MB, Bell JD, Blanchard J, Bonebrake TC, Chen I-C, Clark TD, Colwell**

549   **RK, Danielsen F, Evengård B. 2017.** Biodiversity redistribution under climate change:

550   impacts on ecosystems and human well-being. *Science* **355** (6332), aai9214.

551 **Pennino MG, Arcangeli A, Prado-Fonseca V, Campana I, Pierce GJ, Rotta A, Bellido JM.**

552   **2017.** A spatially explicit risk assessment approach: Cetaceans and marine traffic in the

553   Pelagos Sanctuary (Mediterranean Sea). *PLoS ONE* **12(6)**:e0179686.

554 **Podolsky RH, Kress SW. 1989.** Factors affecting colony formation in Leach's storm-petrel. *The*

555   *Auk* **106:**332-336

556 **Quinn GP, Keough MJ. 2002.** Experimental Design and Data Analysis for Biologists.

557   Cambridge University Press, Cambridge, UK.

558 **Rambaut A, Drummond AJ. 2009.** Tracer version 1.6. Available at http://beast.bio.ed.ac.uk.

559 **R Core Team. 2019.** R: A language and environment for statistical computing. R Foundation for

560   Statistical Computing, Vienna, Austria. URL https://www.R-project.org/.

561 **Sáez A, Cabrera L, Garcés M, Bogaard PVD, Jensen A, Gimeno D. 2012.** The stratigraphic

562   record of changing hyperaridity in the Atacama Desert over the last 10 Ma. *Earth Planet Sci*

563   *Lett* 355–356.

564 **Schmitt F, Barros R, Norambuena HV. 2015.** Markham's Storm Petrel breeding colonies

565   discovered in Chile. *Neotropical Birding* **17**:5–10.

566 **Spear LB, Ainley DG. 2007.** Storm-petrels of the Eastern Pacific Ocean: species assembly and

567   diversity along marine habitat gradients. *Ornithol. Monogr.* 62.

568 **Spiegelhalter D, Best N, Carlin B, van der Linde A. 2002.** Bayesian measures of model

569   complexity and fit. *J. R. Sta.t Soc. Series B Stat. Methodol.* **64**:583–616.

570   **Stamatakis A. 2014.** RAxML version 8: a tool for phylogenetic analysis and post-analysis of

571   large phylogenies. *Bioinformatics* **30**:1312–1313.

572   **Stocker TF, Qin D, Plattner GK, Alexander LV, Allen SK, Bindoff NL, Bréon FM, Church**

573   **JA, Cubasch U, Emori S, Forster P, Friedlingstein P, Gillett N, Gregory JM, Hartmann**

574   **DL, Jansen E, Kirtman B, Knutti R, Krishna-Kumar K, Lemke P, Marotzke J, Masson-**

575   **Delmotte V, Meehl GA, Mokhov II, Piao S, Ramaswamy V, Randall D, Rhein M, Rojas**

576   **M, Sabine C, Shindell C, Talley LD, Vaughan DG, Xie SP. 2013.** Technical Summary. In:

577   Climate Change 2013: The Physical Science Basis. Contribution of Working Group I to the

578   Fifth Assessment Report of the Intergovernmental Panel on Climate Change [Stocker, T.F., D.

579   Qin, G.-K. Plattner, M. Tignor, S.K. Allen, J. Boschung, A. Nauels, Y. Xia, V. Bex and P.M.

580   Midgley (eds.)]. Cambridge University Press, Cambridge, United Kingdom and New York,

581   NY, USA.

582   **Sydeman WJ, Thompson SA, Kitaysky A. 2012.** Seabirds and climate change: roadmap for the

583   future. *Marine Ecology Progress Series* **454**:107–117.

584   **Torres-Mura JC, Lemus ML. 2013.** Breeding of Markham's Storm-Petrel (*Oceanodroma*

585   *markhami*, Aves: Hydrobatidae) in the desert of northern Chile. *Revista Chilena de Historia*

586   *Natural* **86**:497–499.

587   **van Vuuren D, Edmonds J, Kainuma M, Riahi K, Thomson A, Hibbard K, Hurtt GC,**

588   **Kram T, Krey Vr, Lamarque J-F, Masui T, Meinshausen M, Nakicenovic N, Smith SJ,**

589   **Rose SK. 2011.** The representative concentration pathways: an overview. *Climatic Change*

590   **109**:5–31.

591   **Venter O, Sanderson EW, Magrach A, Allan JR, Beher J, Jones KR, Possingham HP,**

592   **Laurance WF, Wood P, Fekete BM, Levy MA, Watson JE. 2016.** Global Terrestrial

593   Human Footprint Maps for 1993 and 2009. *Scientific Data* **3**:160067.

594   https://doi.org/10.1038/sdata.2016.67.

595   **Vieilledent G. 2019.** hSDM: Hierarchical Bayesian Species Distribution Models. R package

596   version 1.4.1. https://CRAN.R-project.org/package=hSDM.

597   **Wallace WJ, Morris-Pocock JA, González-Solís J, Quillfeldt P, Friesen VL. 2017.** A

598   phylogenetic test of sympatric speciation in the Hydrobatinae (Aves: Procellariiformes).

599   *Molecular Phylogenetics and Evolution* **107**:39-47.

600   **Wolf SG, Snyder MA, Sydeman WJ, Doak DF, Croll DA. 2010.** Predicting population

601   consequences of ocean climate change for an ecosystem sentinel, the seabird Cassin's auklet.

602   *Global Change Biology* **16**: 1923−1935.

603   **Xia X, Xie Z, Salemi M, Chen L, Wang Y. 2003.** An index of substitution saturation and its

604   application. *Molecular Phylogenetics and Evolution* **26(1)**:1−7.

605   **Zurell D, Jeltsch F, Dormann CF, Schröder B. 2009.** Static species distribution models in

606   dynamically changing systems: how good can predictions really be? *Ecography* **32**: 733-744.

607   **Zurell D, Thuiller W, Pagel J, Cabral JS, Münkemüller T, Gravel D, Dullinger S, Normand**

608   **S, Schiffers KH, Moore KA, Zimmermann NE. 2016.** Benchmarking novel approaches for

609   modelling species range dynamics. *Global Change Biology* **22**: 2651-2664.

Summary of the fixed effects posterior distribution for the best model of the *H. markhami*.

Table 1. Summary of the fixed effects posterior distribution for the best model of the *H. markhami*. Mean, standard deviation (SD), and a 95% credible interval containing 95% of the probability under the posterior distribution (Q0.025-Q0.975). Bio 6=min temperature of coldest month, Bio 7= temperature Annual Range, Bio 8= mean temperature of wettest quarter, Bio 9= mean temperature of driest quarter. HFP= human footprint.

1   **Table 1**. Summary of the fixed effects posterior distribution for the best model of the *H. markhami*.

2   Mean, standard deviation (SD), and a 95% credible interval containing 95% of the probability

3   under the posterior distribution (Q0.025-Q0.975). Bio 6=min temperature of coldest month, Bio

4   7= temperature Annual Range, Bio 8= mean temperature of wettest quarter, Bio 9= mean

5   temperature of driest quarter. HFP= human footprint.

	Mean	SD	Q0.025	Q0.975
Intercept	-17.732	1.685	-20.571	-14.448
Bio 6	-14.658	4.128	-25.068	-9.147
Bio 7	-5.682	2.525	-10.823	-1.414
Bio 8	5.348	1.902	1.575	9.054
Bio 9	14.750	2.407	10.725	19.674
HFP	1.251	0.539	0.189	2.331
Light	0.524	0.758	-1.023	2.061
Radiation	3.141	2.028	0.179	6.65
Wind	1.595	1.658	-1.241	4.207
Vrho	75.605	3.492	71.218	84.312
Deviance	45.966	9.403	29.630	65.917

Expected change in habitat (number of pixels) by simulation. GCMs= general circulation models , RCP=Representative Concentration Pathway.

Table 2. Expected change in habitat (number of pixels) by simulation. GCMs= general circulation models, RCP=Representative Concentration Pathway. Threshold = value to change a continuous prediction to binary. No Dispersal= number of cells that would be occupied in the case of the No Dispersal scenario. Unlimited Dispersal= Number of cells that would be occupied in the case of the Unlimited Dispersal scenario. Occupied= number of cells that are in an occupied state at the end of the given dispersal step. Absent= Number of cells that are in an unoccupied state at the end of the given dispersal step. Total Colonized= Number of cells that turned into an occupied state. Total Decolonized= Number of cells that turned into an unoccupied state during the given dispersal step.

1   **Table 2**. Expected change in habitat (number of pixels) by simulation. GCMs= general circulation

2   models, RCP=Representative Concentration Pathway. Threshold = value to change a continuous

3   prediction to binary. No Dispersal= number of cells that would be occupied in the case of the No

4   Dispersal scenario. Unlimited Dispersal= Number of cells that would be occupied in the case of

5   the Unlimited Dispersal scenario. Occupied= number of cells that are in an occupied state at the

6   end of the given dispersal step. Absent= Number of cells that are in an unoccupied state at the end

7   of the given dispersal step. Total Colonized= Number of cells that turned into an occupied state.

8   Total Decolonized= Number of cells that turned into an unoccupied state during the given dispersal

9   step.

GCMs	RCP	Threshold	No Dispersal Count	Unlimited Dispersal Count	Occupied Count	Absent Count	Total Colonized	Total Decolonized
	8.5	300	44	966	656	1234864	675	64
	2.6	300	44	909	813	1234707	878	110
CCMA	8.5	500	42	421	390	1235130	405	60
	2.6	500	41	434	414	1235106	433	64
	8.5	700	38	197	195	1235325	190	40
	2.6	700	37	215	209	1235311	201	37
	8.5	300	44	1271	661	1234859	699	83
	2.6	300	44	1073	851	1234669	876	70
CSIRO	8.5	500	42	691	490	1235030	480	35
	2.6	500	42	371	352	1235168	385	78
	8.5	700	37	351	292	1235228	269	22

	2.6	700	35	149	145	1235375	169	69
	8.5	300	43	1140	664	1234856	700	81
MIROC	2.6	300	44	1227	916	1234604	923	52
	8.5	500	42	580	431	1235089	487	101
	2.6	500	42	587	471	1235049	439	13
	8.5	700	37	228	196	1235324	255	104
	2.6	700	36	276	202	1235318	178	21

Figure 1

Map of the phylogeographic structure of *Hydrobates markhami*

Map of the phylogeographic structure of *Hydrobates markhami* showing: (A) the mtDNA ND1 Bayesian Inference (BI) and Maximum Likelihood (ML) phylogeny and the distribution of the three main clades (Upper node values represent BI posterior probabilities and down nodes values represent ML bootstrap values). (B) Haplotype network and each locality; the scale represents the sample size for each locality. At the bottom is the map with the breeding sites used for the genetics analysis. Out-groups on phylogeny are not shown. Photograph of *H. markhami*: courtesy of Fernando Díaz Segovia.
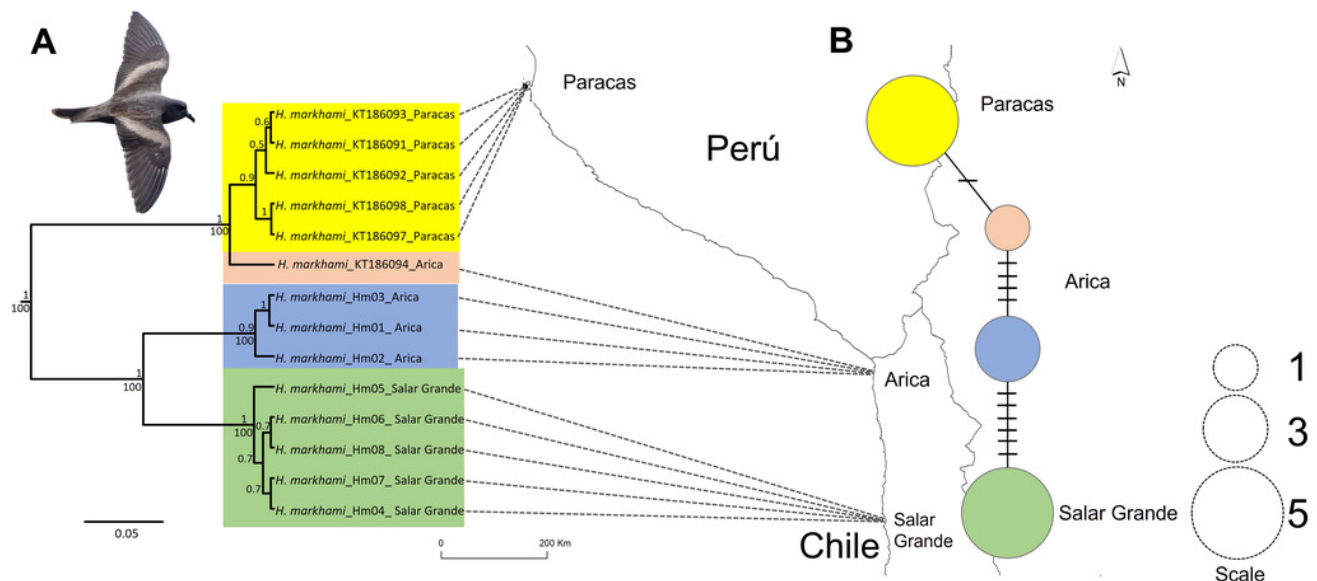
Figure 2

A) Median of the posterior probability of the presence of the *Hydrobates markhami*, B) Spatial effect (the spatial component represents the intrinsic spatial variability of the data without variables).
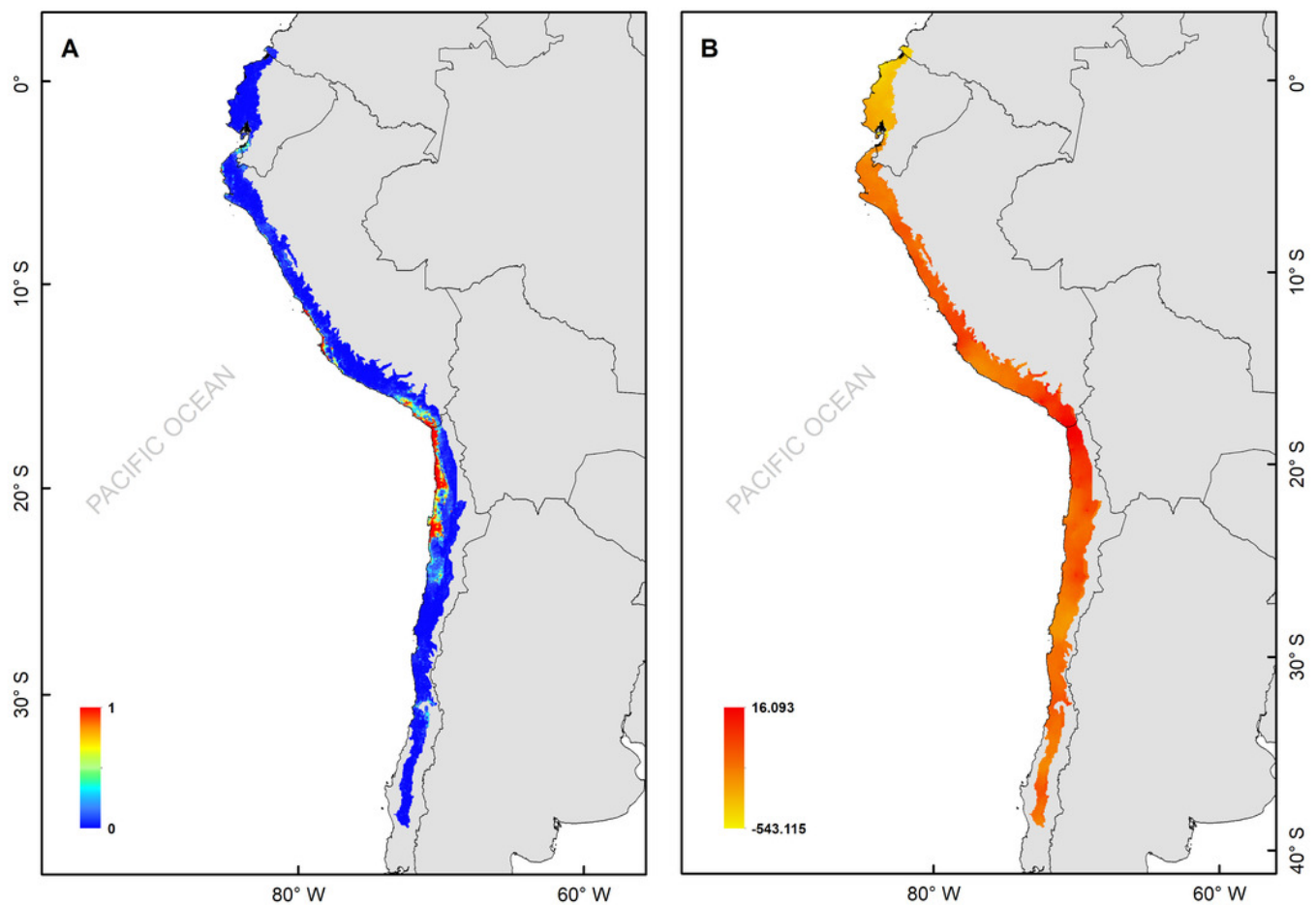
Figure 3

Habitat suitability maps for future climatic conditions predicted for 2080 under a RCP 2.6 (benign scenario).

A) Map of habitat suitability under GCMs CCCMA B) Map of habitat suitability under GCMs CSIRO, and C) Map of habitat suitability under GCMs MIROC.
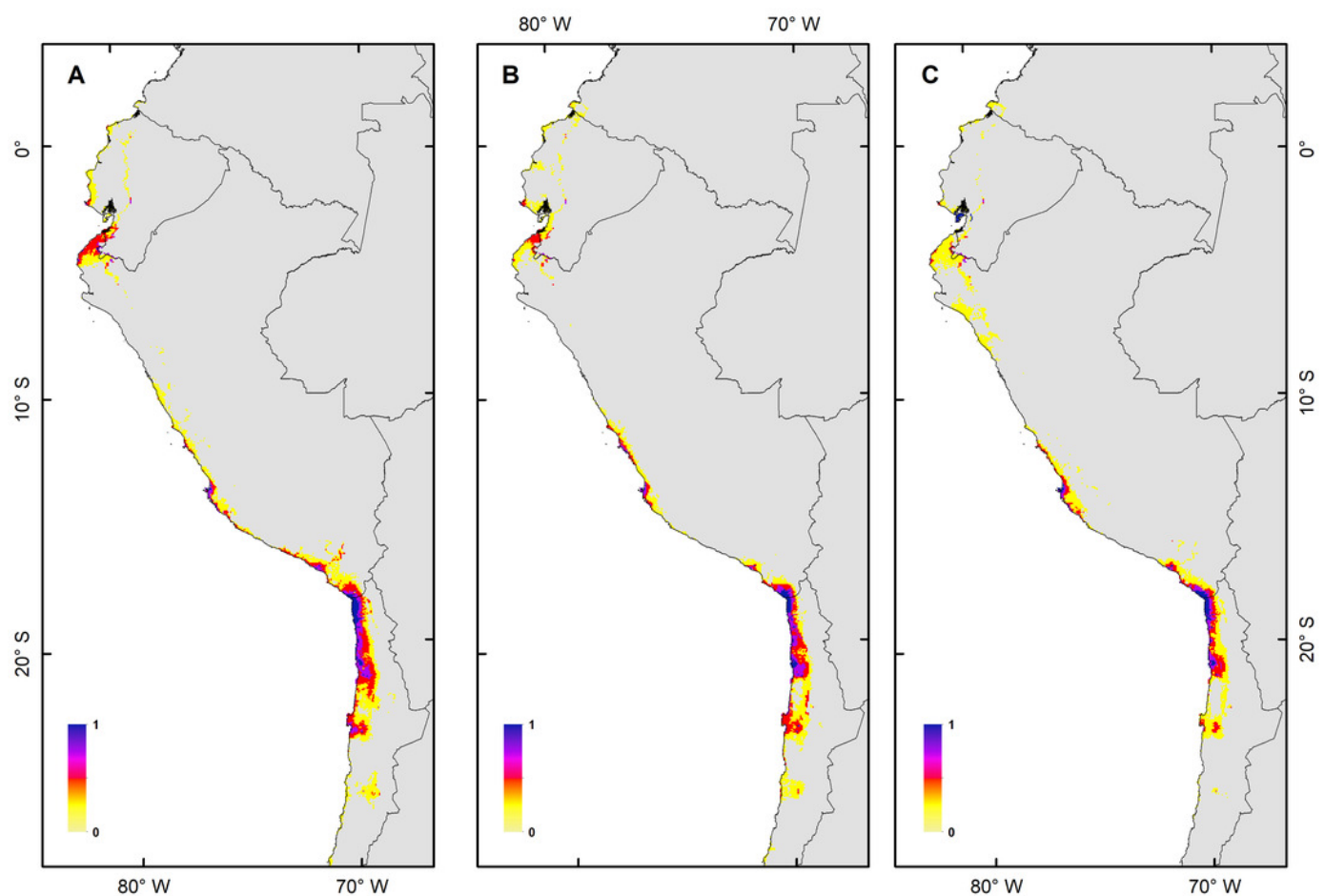
Figure 4

Habitat suitability maps for future climatic conditions predicted for 2080 under a RCP 8.5 (hard stage).

A) Map of habitat suitability under GCMs CCCMA, B) Map of habitat suitability under GCMs CSIRO, and C) Map of habitat suitability under GCMs MIROC.
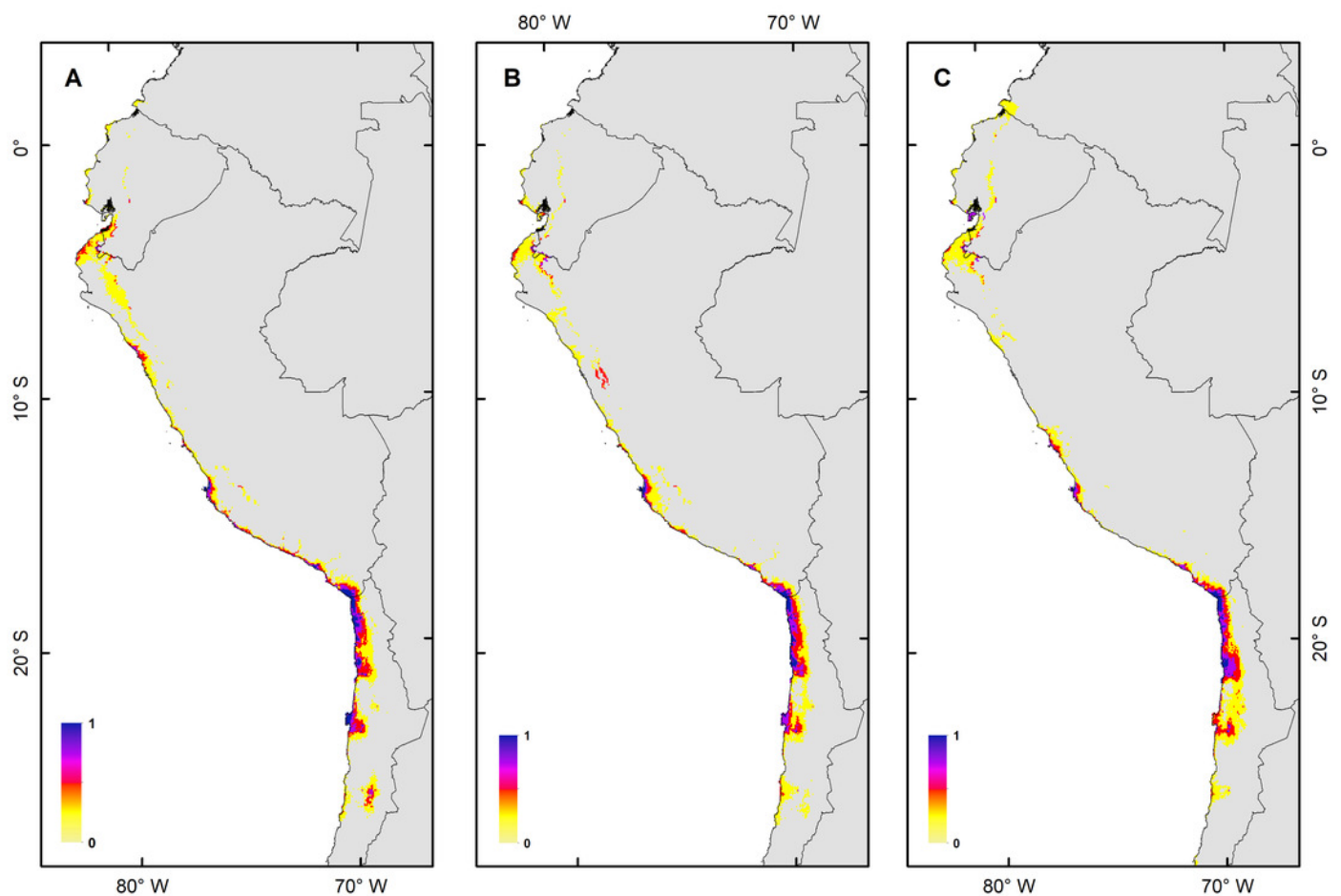
Figure 5

MIGCLIM output map Dispersal restricted future distribution of *Hydrobates markhami*, under two RCP.

A) Simulation for model MIROC (RCP 2.6). B) Simulation for model CCCMA (RCP 8.5).

A

B

Ecuador

Peru

PACIFIC OCEAN

Peru

Peru

PACIFIC OCEAN

PACIFIC OCEAN

Peru

Perú

Chile

PACIFIC OCEAN

Peru

Bolivia

Chile

PACIFIC OCEAN

Chile

PACIFIC OCEAN

Pixels that were once occupied but turned
unsuitable after environmental change

Pixel that have never been occupied and are unsuitable at
the end of the simulation.

Pixels of the species initial distribution that remained
suitable throughout the simulation

Pixels that have been colonized during the simulation and
that remain occupied at the end of the simulation

Suitable pixel that could not be colonized